11-1-2022

Cyclic Porewater Pressure Generation in Intact Silty Soils

Arash Khosravifar
Portland State University, karash@pdx.edu

Stephen Dickenson

Diane Moug
Portland State University, dmoug@pdx.edu

Citation Details

Published as: Khosravifar, A., Dickenson, S., & Moug, D. (2022). Cyclic porewater pressure generation in intact silty soils. Soil Dynamics and Earthquake Engineering, 162, 107482.

Cyclic Porewater Pressure Generation in Intact Silty Soils

Arash Khosravifar[1,*], Stephen Dickenson[2], Diane Moug[3]

[1] *Assistant Professor, Department of Civil and Environmental Engineering, Portland State University, Portland, OR 97201; e-mail: karash@pdx.edu*
[2] *Principal Engineer, New Albion Geotechnical, Inc., Reno, NV 89509; e-mail: sed@newalbiongeotechnical.com*
[3] *Assistant Professor, Department of Civil and Environmental Engineering, Portland State University, Portland, OR 97201; e-mail: dmoug@pdx.edu*

ABSTRACT

The results of cyclic strain-controlled, constant volume direct simple shear (CDSS) tests and field shaking tests have been evaluated for intact, natural, low-plastic silts from six different fine-grained soils with 54% to 100% fines content, 47% to 83% silt content, and plasticity indices (PI) ranging from nonplastic to 16. These tests constitute a subset of a larger archive of CDSS tests performed on silt deposits from the Pacific Northwest, British Columbia, and Alaska collected and analyzed by the co-authors. The cyclic data are presented in this paper for two objectives: (a) to characterize cyclically-induced excess pore pressure generation in intermediate soils with various soil index properties and stress histories, and (b) to provide calibrated Vucetic and Dobry model parameters for simulating excess pore pressure generation in the silt soils based on the data and trends presented in the first objective. The CDSS test results showed that excess pore pressure ratios decrease with PI over the narrow range of PI evaluated and decrease with overconsolidation ratio. The cyclic threshold shear strain amplitude for pore pressure generation extracted from field shaking tests on silts were within the range proposed in the literature, confirming that the cyclic threshold shear strain amplitude is a fundamental soil property. Calibrated Vucetic and Dobry model parameters for these intermediate, fine-grained silts were

* Corresponding author.
E-mail address: karash@pdx.edu (A. Khosravifar)

significantly different than those reported for sands in the literature and were heavily influenced by the overconsolidation ratio. The calibrated parameters obtained in this study can be used as a benchmark in selecting model parameters for silts.

Keywords: Cyclic behavior of silts, cyclic pore water pressure, strain-controlled CDSS, intermediate soils

1 INTRODUCTION

Silt-rich soil deposits are prevalent in the Pacific Northwest region of the USA as well as other parts of the world. While the majority of past research has been focused on the cyclic behavior of sands and clays, few studies have investigated the cyclic response of intermediate fine-grained soils that fall in between classical sand and clay types. The cyclic behavior of silt has been documented as intermediate between the generalized and short-hand characterization of soil behavior as either “sand-like” or “clay-like”, thereby adding a level of complexity to seismic vulnerability studies involving silt.

Several studies have investigated the effects of fines content (FC) on cyclic strength of silty sands, and the conclusions of these studies vary. While some studies report that the cyclic strength of soils decreases with increasing FC (e.g. Shen et al. 1977, Troncoso and Verdugo 1985, Vaid 1994), other studies report that cyclic resistance decreases up to a limiting silt content beyond which the cyclic strength increases with FC (e.g. Koester 1994, Polito and Martin 2001). Polito and Martin (2001) found that this limiting silt content—where the soil behavior transitions from being governed by its coarse fraction to being governed by its fine fraction—ranges between 25% to 40% for most soils. Hazirbaba and Rathje (2009) reported that the excess pore pressure of sand decreases (i.e., equivalent to an increase in cyclic resistance) up to a FC of 10%; beyond that point, it either levels off or increases for FC up to 20%. A similar trend was reported by Mousavi and Ghayoomi (2020). The abovementioned studies focus on sands with non-plastic fines, and most were based on testing programs using reconstituted samples.

While tests on reconstituted samples aid in understanding the fundamental soil behavior on close-to-identical specimens, the implications of the findings for naturally deposited soils need to be investigated. This is particularly important, as naturally deposited soils with higher FC also tend to have a higher PI (Mitchell and Soga 2005). As shown by the results of many studies, the cyclic resistance of soils tends to increase with PI (e.g., Bray and Sancio 2006, Idriss and Boulanger 2006). A number of studies have investigated the cyclic resistance of silts with respect to PI using stress-controlled cyclic shear tests on intact specimens (e.g., Dahl et al. 2014, 2018; Wijewickreme et al. 2019). While stress-controlled tests are useful in characterizing the cyclic shear resistance for “triggering liquefaction”, defined as pore pressure ratios of ~100% or some level of large shear strain (e.g., 3.0 to 3.75%), strain-controlled tests are often used to characterize the development of excess pore pressure with loading cycles over a range of shear strain amplitudes. In a few studies, strain-controlled tests were conducted to characterize the pore pressure generation of intact plastic silt specimens with PIs ranging from 17 to 39 (Jana and Stuedlein 2021); however, very little published data can be found on pore pressure generation of low plasticity silts in strain-controlled cyclic shear tests. The study presented here attempts to fill this gap by reporting on strain-controlled cyclic shear tests performed on natural, intact, low-plasticity silts with PIs ranging from nonplastic (NP) to 16. The results of the study have practical implications, considering that the cyclic behavior of fine-grained soils that fall in this range of PI may be characterized differently based on commonly used screening methods (e.g., Bray and Sancio 2006, Idriss and Boulanger 2008).

The first objective of this study is to evaluate excess pore pressure generation as a function of the following soil characteristics; soil index properties (e.g., FC, Atterberg limits, silt and clay contents, interfine void ratio, and gradation) and stress history (overconsolidation ratio, OCR). Data from cyclic Direct Simple Shear (CDSS) tests on intact samples from six engineering project sites in Oregon and Washington has been evaluated. The soils were obtained from different coastal marine environments and fluvial depositional environments, including riverine and estuarine/tidal. The second objective of the study is to provide calibrated Vucetic and Dobry model (Vucetic and Dobry 1986; Matasović 1993; Matasović and Vucetic 1993) parameters (hereafter referred to as V&D) for the tests presented in this paper. The V&D model is one of several available constitutive models to simulate cyclic pore pressures in soils and is a focus of this study because of its widespread use in effective-stress site response analysis tools, and because it provides a means to evaluate excess pore pressure tendencies with varying cyclic shear strain and loading cycles. The V&D model parameters developed for silt soils in this study are compared to model parameters presented for sand soils in other studies to highlight the difference between excess pore pressure generation in sands and low-plasticity silts. Finally, a set of predictive equations are provided as a benchmark for practitioners to use when selecting constitutive model parameters for silt-rich soils.

2 DATA USED IN THIS STUDY

2.1 Soil Classification & Index Properties

The dataset presented in this study includes 35 strain-controlled constant volume direct simple shear (CDSS) tests and a series of field shaking tests using truck-mounted shakers from the NHERI@UTexas facility at the University of Texas at Austin. Additionally, data from six stress-controlled CDSS tests are included where the data were analyzed by McCullough et al. (2009) using procedures by Matasović and Vucetic (1993) to interpret pore water pressures at average shear strain amplitudes to be comparable to strain-controlled test data. The tests are performed on intact natural soils from six sites characterized as representative of different depositional environments (alluvial, fluvial, and tidal/estuarine). Table 1 lists key soil properties and test parameters.

The majority of the soils collected are fine grained and are characterized as low-plasticity silt (ML), low-plasticity clay (CL), or low-plasticity silty clay (CL-ML) based on their USCS classification. The focus in this study is on silt-rich soils with fines content ranging from 54% to 100%, silt content ranging from 47% to 83%, and PI ranging from NP to 16. Additionally, six strain-controlled CDSS tests on sands (SP) and silty sand soils (SM) with FC ranging between 1% and 31% are included from a site in coastal Washington (Table 1 – Project W_01). These tests helped highlight the differences between pore pressure generation tendencies in sands and silts. The plasticity characteristics of the soils evaluated in this study are plotted in Figure 1a. Figure 1b shows that the soils presented in this study are characterized as being susceptible to liquefaction or cyclic softening based on screening methods by Idriss and Boulanger (2008) using the illustration method developed by Armstrong and Malvick (2016). It is important to note that the PI of these natural deposits tends to increase with increasing FC, as shown in Figure 1b. This will be later used to highlight some of the differences between the findings in this study and the results of other studies of sand mixtures that contain a nonplastic silt.

2.2 Cyclic Testing

The CDSS tests were performed under constant-volume conditions and the pore pressures were back-calculated from the change in vertical stress. The cyclic shear strain amplitudes (hereafter referred to as cyclic shear strain) in the strain-controlled CDSS tests ranged from 0.1% to 2%. The cyclic loading in CDSS tests was applied mostly at a frequency of 0.1 Hz except for the tests performed at the University of California at Los Angeles for the tidal/estuarine silt deposits in Washington (Project W_03), in which the loading frequency was varied between 0.01 Hz and 0.1 Hz. The field shaking tests (Project O_24) by Stokoe et al. (2020) were performed with a loading frequency from the truck shakers of 10 Hz. Various studies have shown the strain rate effects (frequency of loading) on the cyclic resistance and porewater pressure buildup in fine-grained soils. For example, Mortezaie and Vucetic (2013) showed that cyclic porewater pressures consistently increase as the loading frequency is decreased. Therefore, the few data points from Projects W_03 and O_24 where the loading frequencies were different than 0.1 Hz used in the rest of the dataset might be affected by the strain rate effects; however, the conclusions and overall trends are not believed to be affected by these data points. In most cases, the CDSS data were supplemented with bender element shear wave velocity (V_s) measurements performed after consolidation and immediately prior to cyclic loading. The specimens in the CDSS tests were consolidated to a vertical effective stress that was slightly larger than the in-situ vertical effective stress to reduce the effect of sample disturbance (a factor of 1.2 for specimens in Projects W_01 and O_01 and factors ranging between 1 and 3.8 for other projects in this database). The field shaking included crosshole V_s measurements prior to cyclic loading.

2.3 Sample Quality Assessment

Several approaches were used to evaluate sample quality on intact specimens. A summary of the available data and sample quality assessment is provided in Table 2. Detailed descriptions of sample quality assessment for different projects and methods used are provided in Appendix A. Overall, the available data from projects O_15, W_01, and W_08 indicate that sample disturbance was minimized. There are no available data to evaluate the disturbance of samples tested for project W_03, however, the project's data report details that Shelby tube sampling was performed with mud rotary drilling and an Osterberg sampler, where these approaches are considered to reduce sample disturbance of fine-grained soils. Samples from O_01 are considered poor quality which likely impacts the laboratory-characterized cyclic behavior.

3 CORRELATIONS BETWEEN CYCLICALLY INDUCED PORE PRESSURES AND SOIL INDEX PROPERTIES

3.1 Effects of Gradation, Plasticity, Void Ratio, and Shear Wave Velocity on Excess Pore Pressures

Figure 2 shows the variation of cyclically induced porewater pressure ratio with the number of uniform loading cycles at a constant cyclic shear strain of γ_c = 0.1%—where the porewater pressure ratio is defined as the residual excess porewater pressure at the end of each loading cycle normalized by the initial vertical stress prior to cyclic loading (i.e., R_u = $\Delta u/\sigma'_{vo}$). The trend shows an increasing porewater pressure ratio with the number of cycles. The sand material (SP) generated significantly larger pore pressures compared to those of fine-grained materials (ML, CL, and CL-ML). The variation of R_u and various soil properties are investigated for silt-rich soils in the next section by comparing the R_u values at 30 cycles (N = 30). The 30th cycle is selected only as a reference since, in most tests, the R_u values start to plateau at about 30 cycles. It is worth noting that a cycle number ranging between 15 to 30 is typically used in laboratory tests to represent the equivalent number of cycles for a magnitude 7.5 earthquake loading for sand-like and clay-like soils (Idriss and Boulanger 2008).

Figure 3 shows the possible correlations, or lack thereof, between R_u at a cyclic shear strain of γ_c = 0.1% after 30 loading cycles with various soil properties. These soil properties are selected based on commonly used screening methods that adopt different combinations of soil properties (e.g., FC, silt content, clay content, PI, liquid limit (LL), ratio of water content to LL (w_c/LL), interfine contact void ratio, and V_s) as indicators to assess the potential for liquefaction and cyclic softening in silts (e.g., Wang, 1979, Ishihara 1993, Youd 1998, Polito and Martin 2001, Andrus and Stokoe 2000, Seed et al. 2003, Wang et al. 2006, Boulanger and Idriss 2006, Bray and Sancio 2006, and Thevanayagam 2007). However, it is important to note that the trends shown in Figure 3 present the development of R_u with cyclic loading at low to moderate shear strains (e.g. γ=0.1%), which is not directly comparable to liquefaction triggering correlations that are based on high levels of pore pressures (i.e. R_u=100%) and/or large shear strains (i.e. γ=3%).

The variation between R_u and FC in Figure 3a illustrates that for soils with FC>30%, the excess pore pressure decreases as FC increases. A similar decreasing trend is observed between R_u and the silt content (i.e., particle size between 0.075 mm and 0.005 mm) and clay content (i.e., particle size smaller than 0.005 mm) as shown in Figures 3b and 3c, respectively. It is speculated that the decreasing trend between R_u and fines/silt/clay content for the natural silts in this study is related to other fundamental soil characteristics such as soil plasticity. The plot presented in Figure 3d shows a decreasing trend between R_u and PI. The NP soils are plotted at PI = 0; however, due to uncertainties in measuring Atterberg limits for soils with very low plasticity, their PI values could be somewhat larger (up to PI ~4). The variations of R_u with LL and w_c/LL are shown in Fig. 3e and Fig. 3f, respectively (excluding the two NP soils). These two variables do not appear to have an effect on R_u for the range of data in this study with LL>27 and w_c/LL>0.99.

Figure 3g shows an increasing trend between R_u and interfine contact void ratio (e_f). e_f is defined based on the global void ratio (e) and FC using the equation below and has been shown by some studies to relate to liquefaction resistance of soil mixtures where the fine grain contact dominates the cyclic response (e.g., Thevanayagam 2007):

$$e_f = \frac{e}{FC} \tag{1}$$

Figure 3h shows the lack of strong correlation between R_u and $V_{s,lab}$ for fine-grained soils data in this study. Some studies have shown that the grain size distribution of sand soils affects their tendency to develop cyclic excess pore pressures. For example, Li (2013) showed that excess pore pressures increase with an increasing coefficient of uniformity (Cu) for Houston Sand. Similarly, Mei et al. (2018) calibrated V&D model parameters for different sands and showed that Parameter F in the V&D model increases with Cu, indicating an increasing tendency to develop excess pore pressures, as addressed in Section 4. In contrast, the data for silt-rich soils used in this study show a decreasing trend between R_u and Cu, as shown in Figure 3i. While some of the soil properties plotted in Figure 3 serve as indicators for decreasing or increasing trends in R_u, no single soil property was found to explain all aspects of the observed experimental data. This observation may be attributed to the inherent variabilities in characteristics of natural soils not captured using the soil parameters applied in Figure 3 (e.g., grain shape, inclusion of biogenic grains, fabric, aging), and the sampling and testing procedures performed in different projects.

The relationships between R_u and various soil properties were evaluated at larger cyclic shear strains as well. Figures 4a and 4b show the variation of R_u with the number of loading cycles for cyclic tests performed at constant shear strains of 0.4% and 1.6%, respectively. The results show similar trends to those observed for the tests at 0.1% shear strain, i.e., the sand material (SP) developed considerably higher R_u as compared to the silts and silty soils, even in the first few cycles of loading. The R_u values generally decrease as the PI and FC increase in silts and silty soils (SM, ML, CL). Figures 5a and 5b show R_u for the tests that reached 30 uniform loading cycles at constant shear strains of 0.4% and 1.6% with respect to PI. While the R_u values appear to decrease with increasing PI, the correlation becomes less strong at larger shear strains as the R_u values appear to approach their theoretical maximum value of 100%. The data points corresponding to the fluvial soils with PI of 10 and FC of 60% from Tacoma, Washington (Project W_08) produced noticeably smaller R_u values compared to other specimens from the same soil unit and other soils with similar PI. It is speculated that these samples were slightly overconsolidated, as they were obtained from relatively shallow depths (5 m). The effect of overconsolidation and stress history on porewater pressure generation is discussed in the next section. The scatter in data highlights the importance of accounting for the inherent variability in the estimated pore pressures due to uncertainties in soil properties (e.g., PI and OCR).

3.2 Effects of Stress History on Excess Pore Pressures

The tests performed on overconsolidated (OC) samples exhibited noticeably smaller porewater pressures compared to normally consolidated samples (NC). The results shown in Figure 6 were obtained from nine strain-controlled CDSS tests performed on Willamette Silt samples from Project O_15 with relatively similar plasticity (PI ranging from 5 to 9). The samples were first consolidated to a confining stress larger than their preconsolidation stress and then unloaded to a lower stress to produce overconsolidation ratios (OCRs) of 1.5 and 2.5. The specimens prepared at OCR = 2.5 showed negative to negligible R_u values at shear strains of 0.1% and

0.4%, and they developed a positive R_u value of 78% at a relatively large shear strain of 2% after 60 cycles of loading. This observation is consistent with the findings of other researchers where the cyclic porewater pressure ratios first decreased with the number of loading cycles at small cyclic shear strains (0.74%) and then increased at larger shear strains (1.68%) in OC clays (e.g., Dobry and Vucetic 1987 and Vucetic 1988). While some differences in R_u values in Figure 6 could be due to small variations in PI (ranging between 5 and 9) the primary reason for significantly different R_u values in this figure is attributed to the differences in OCR.

3.3 Summary of Excess Pore Pressures in NC and OC Silts

Figure 7 summarizes the R_u values from NC and OC tests on intact, natural silt-rich soils in the database used in this study. For consistency, all R_u values are compared for cyclic shear strain of 0.1% after 30 loading cycles. The R_u values are plotted against FC in this figure to enable them to be compared to the results obtained in other strain-controlled tests performed on sands and silty sands. The observed range of R_u values clearly shows the effect of OCR in decreasing cyclically induced pore pressures. Several supplemental data points from this study (SP and SM soils in Project W_01 and ML soils in Project O_24) and other studies (Jana and Stuedlein 2021) that were added to this figure confirm the observed trends between R_u and FC, and R_u and OCR. The field shaking tests on Columbia River Silt (Project O_24) correspond to soils with PI of 13 and OCR ranging from 2.1 to 3 for soils at depths ranging from 1.55 m to 2.55 m. The field shaking tests consisted of sequential tests with increasing amplitude. The subset of data presented in this figure corresponds to shaking events that produced shear strain values close to 0.1% (ranging from 0.08% to 0.12%). The field shakings correspond to N = 36 cycles at 10 Hz. More details on the field shaking tests are provided in Stokoe et al. (2020) and Preciado et al. (2021). The field shaking tests data fall within the range of observed values from CDSS tests on OC samples. An additional data point from CDSS tests on intact natural alluvial silts from Columbia River in Portland basin with PI = 26 and OCR from 1.8 to 2 by Jana and Stuedlein (2021) is plotted for comparison purposes; this data point also falls within the range observed for the OC specimens in this study. The PI value for every data point is shown to emphasize that the natural soils in this study have different plasticity indices, and this might contribute to the scatter in the data.

The decreasing trend between R_u and FC in this study generally agrees with the results of other studies that used reconstituted sand mixtures with non-plastic silt (e.g., Hazirbaba and Rathje 2009). The data in this study expand upon these findings by examining natural silts which tend to be less dilative than mixtures composed of crushed silica for non-plastic fines, and intact specimens that maintain some natural soil fabric and cementation. Additionally, the soils examined in this study provide insight into trends of how R_u relates to FC for FC greater than 30% and varying PI and how R_u relates to OCR. The observed trends between R_u and FC, PI, and OCR shown in Figures 3 to 7 are used as a basis for calibrating V&D parameters for silt soils in the next section.

4 CALIBRATION OF V&D MODEL PARAMETERS FOR SILTS

The second objective of this study is to provide calibrated intermediate soil model parameters for the Vucetic and Dobry (1986) strain-based pore pressure model for sand (i.e., the V&D model) to estimate cyclically induced pore pressures at different numbers of uniform loading cycles and at different shear strain levels. The V&D models are commonly used in practice in effective-stress site response analysis using software programs such as DEEPSOIL (Hashash et al. 2020), D-MOD (Matasović and Vucetic 1995) and D-MOD2000 (Matasović and Ordonez 2012). Olson et al. (2020) showed that using the V&D pore-pressure model in combination with the cyclic stress-strain constitutive model of Groholski et al. (2016) was effective for estimating excess pore pressures in effective-stress site response analysis. The model parameters for V&D sand and clay models are primarily provided in the literature for sand and clay materials, e.g., Dobry et al. (1985), Vucetic (1986), Thilakarante and Vucetic (1987), Vucetic and Dobry (1988), Matasović (1993), Matasović and Vucetic (1993), Matasović and Vucetic (1995), and Mei et al. (2018).

Despite the wide use of these models in practice, only a few studies have provided model parameters for silts and silty sands, e.g. Thilakarante and Vucetic (1987), McCullough et al. (2009), and Anderson et al. (2010). Due to the scarcity of data on pore pressure generation in silt-rich soils, the V&D model parameters that are developed primarily for sands are often used by practitioners to evaluate the undrained cyclic response and the pore pressure development tendency of silt-rich soils, particularly when the soils are characterized as susceptible to liquefaction or cyclic softening using screening methods such as those in Idriss and Boulanger (2008) and Bray and Sancio (2006). However, using model parameters that are developed for sands tends to result in an overestimation of the pore pressures in silts as shown by Hazirbaba and Rathje (2009), thereby resulting in an over-softening of the dynamic response of silt layers in one-dimensional effective-stress site response analysis.

To address this issue, the V&D model parameters in this study are calibrated using strain-controlled tests on primarily intact, natural silts, as described in the previous section. The calibrated V&D model parameters for silts in this study are compared with those reported in the literature for sands to illustrate the differences between pore pressure development tendencies in sands and silts. Correlations between calibrated model parameters and various soil properties are investigated, and a set of predictive models are proposed to estimate V&D model parameters for silts. An evaluation of the effectiveness of the V&D model for predicting pore pressures in silty soils using the proposed predictive equations is also provided. The V&D parameters that are provided in this paper serve as a reference for practitioners in modeling cyclic behavior of low plasticity silts. It is noteworthy that the V&D sand model is one of the many models that are available for strain-based effective-stress site response analysis (e.g., Green et al. 2000). The V&D model is used in this study since it is widely used in engineering practice.

4.1 Calibration Procedures

The V&D model for sands was fit to the lab data presented in this study. The model equation is provided in Equation (2). Details on the model parameters can be found in Dobry et al. (1985), Vucetic and Dobry (1986), Vucetic (1986), Matasović (1993) and Matasović and Vucetic (1993).

$$R_u = \frac{PfNF\left(\gamma_c - \gamma_{tvp}\right)^s}{1 + fNF\left(\gamma_c - \gamma_{tvp}\right)^s} \tag{2}$$

where R_u is defined as the residual pore pressure ratio after N cycles of loading at a constant shear strain of γ_c. The f value in Eq. (2) accounts for the direction of loading. The objective in this study is to calibrate the model parameters to data from lab tests that were all performed under unidirectional loading; therefore, f = 1 was used in this study. Parameters F, s, and P were calibrated based on curve fitting procedures described in Vucetic (1986), Matasović and Vucetic (1993), and Mei et al. (2018). While the P and F parameters reported in this paper are derived from the curve fitting procedures described in the above references, in most cases, s was defined by iterative adjustment to produce the best fit between the measured and predicted pore pressures, as suggested by Matasović and Vucetic (1993). The cyclic threshold shear strain amplitude for volumetric strain (γ_{tvp}) (hereafter referred to as threshold shear strain) was selected using the middle curve proposed by Mortezaie and Vucetic (2016), which will be shown to reasonably envelop the data from this study and other studies on silts.

Figure 8 shows an example comparison between lab-measured and model-predicted R_u values for three strain-controlled CDSS tests performed on Willamette Silt samples (Project O_15). The tests were performed at shear strains of γ_c = 0.1%, 0.4%, and 1.6% on specimens consolidated to vertical effective stresses of 240 kPa. These specimens had FC of 99%, silt content of 79%, LL of 30, PI of 9, and water contents ranging between 32% and 36%. These samples are characterized as susceptible to liquefaction and/or cyclic softening based on screening procedures often used in practice (e.g., Bray and Sancio 2006, Idriss and Boulanger 2008). Figure 8a shows R_u versus cyclic shear strain for lab data (indicated as symbols) and the calibrated V&D model (indicated as solid lines). Figure 8b shows R_u versus loading cycles from the CDSS tests and the calibrated V&D model. Variability in the trends of measured and predicted Ru with number of loading cycles is noted for each cyclic shear strain amplitude, therefore it is important to note that the V&D model parameters should be selected by the user to target a specific range of loading cycles and/or shear strains based on project-specific seismic demands. For the calibration performed in this study, the calibrated V&D model reasonably captures the excess pore pressures at larger shear strains (i.e. γ_c = 1.6%) and generally performs better for loading cycles greater than 5.

The calibrated V&D parameters for all the tests and sites in this study, which are listed in Table 3, provide a benchmark for the selection of V&D model parameters in project-specific applications. A comparison between the lab-measured and model-predicted R_u values for all tests in this study is presented in Supplemental Appendix B. In the following sections, the potential correlations, or lack thereof, between V&D model parameters (F, s, P, and γ_{tvp}) and other soil properties (OCR, FC, and V_s) are evaluated.

4.2 Variations between *F* Parameter and Fines Content

Parameter F in the V&D model is the primary variable that controls the tendency for a soil to develop excess pore water pressure during cyclic loading (i.e., larger F values correspond to larger R_u at a given cyclic shear strain). As shown previously in Figures 3 and 7, the soil tendency to develop excess pore pressure decreases as FC increases. Therefore, it is expected that calibrated F parameters should also decrease as FC increases. Figure 9a shows the variation of the calibrated F parameter with FC. Data from this study is supplemented by data from other sandy soils reported in other studies: Banding Sand reported by Dobry et al. (1985), Wildlife Site Sand A and B and Herber Road Site Sand PB and CF reported by Vucetic and Dobry (1988), Santa Monica Beach Sand reported by Matasović and Vucetic (1993), and Owi Island Sand reported by Thilakarante and Vucetic (1987). Several previous studies have shown that the cyclic behavior of a soil mixture transitions from being governed by the coarse fraction to being governed by the fines fraction at FC ranging between 35% and 50% (Polito and Martin 2001, Thevanayagam et al. 2002, Mitchell and Soga 2005). Similarly, Figure 9a illustrates a transition in pore pressure generation tendency (indicated by Parameter *F*) at FC between 40% and 50%. While the *F* parameters for sand soils (FC<40% for the data in this figure) range from 0.75 to 10.9 (mean F = 2.3) the *F* parameters for silt soils (FC>50%) are significantly smaller and range from 0.3 to 1.1 (mean F_{NC} = 0.7).

The comparison between the calibrated *F* parameters for sand soils and silt soils suggests, as expected, that the V&D model parameters developed for sands are not suitable for predicting the pore pressure generation in silts. The analysis in this investigation did not show a strong correlation between *F* and other fundamental soil properties such as PI. Therefore, the trends suggest that a constant value of F_{NC} = 0.7 can be considered for NC silt soils with FC>50% until future refinements can be made as more data become available.

4.3 Variations between *s* Parameter and Fines Content

Parameter *s* in the V&D sand model affects the slope and curvature of the relationship between pore pressure ratio and cyclic shear strain. The relationship between parameter *s* and FC for silt data from this study are compared to that of sand data from other studies in Figure 9b. While the *s* parameter ranges between 1 and 1.8 for sand soils, it is common to use a value of 1 for clean sand with FC < 5% (e.g. Mei et al. 2018). The difference in trends between sand and silt specimens is evident, with data from silt soils in this study (FC greater than 50%) showing *s* values much larger than 1 (and up to 2) for intact, natural NC specimens. The silt data suggests a slightly increasing trend between parameter *s* and FC. As a supplementary trend, the relationship between parameter *s* and FC proposed by Carlton (2014) is also plotted in this figure which confirms an increasing trend between parameter *s* and FC. This is expected, considering that

Carlton's relationship was developed based on data reported in the literature for sands and three data points on silts with FC>50%, which are all included in this study as well.

4.4 Effects of Overconsolidation Ratio on Calibrated *F*, *s*, and *P* Parameters

The effects of stress history (OCR) on the parameters *F*, *s*, and *P* are shown in Figure 10. The plots in this figure include data from a series of tests performed on intact Willamette Silt specimens (Project O_15), where the specimens were consolidated in the lab to OCR values of 1, 1.5, and 2.5. The figure also includes data from field shaking tests conducted on Columbia River Silt (Project O_24) with OCR ranging between 2.1 and 3 (corresponding to the depths of embedded pore pressure sensors). Since the shear strains in the field shaking tests were relatively small (<0.25%), curve fitting for the purpose of calibrating V&D parameters could not be fully constrained at large strains; therefore, a range of calibrated parameters were developed that envelop the measured pore pressures (shown with vertical bars in the figure). While the focus in this paper is on intact specimens, supplemental data from a series of tests on reconstituted samples from estuarine/tidal silts (Project W_04) consolidated to OCR of 1.2 are also included in this figure. Overall, the data in these figures show a decreasing trend between *F* and OCR and an increasing trend between *s* and OCR. Parameter *P* in the V&D model defines the maximum R_u at large shear strains and a large number of loading cycles, somewhat comparable to the R_u values shown previously in Figure 5b (which correspond to a cyclic shear strain of 1.6% and N = 30). The back-calculated *P* parameter for NC silts ranged between 0.94 and 1.0 and did not show a strong correlation with other soil properties for NC silts. However, as shown in Figure 10c, *P* exhibited a decreasing trend with OCR for OC silts.

4.5 Variation Between *F* parameter and Shear Wave Velocity

Carlton (2014) used available data for sand to develop a relationship between *F* parameter and V_s. Figure 11 provides a comparison of Carlton's equation in estimating the *F* parameter for silt soils in this study as well as that for sand soils reported by others. The V_s values for the data points in this study were measured using bender elements in the CDSS device. The significant variability in the silt data precludes a reliable best-fit trendline. It is apparent that the correlation seems to be consistently poor for both sand and silt soils. The *F* parameters for OC soils are well below the estimated values from Carlton's equation. Similar observations were made by Mei et al. (2018) regarding the comparison between Carlton's equation with V_s data for sands. It is also noted that the two sand data points in this study (SP and SM soils from Project W_01) exhibited noticeably larger *F* values compared to those of silt soils (ML, CL and CL-ML) having similar V_s values. This finding indicates a higher susceptibility to pore pressure generation for sand soils than for silt soils having similar V_s values. It is important to note that the study presented here evaluates the rate of progressive excess pore pressure generation during cyclic loading (using F parameter as a proxy), which is not directly comparable to V_s-based correlations to predict liquefaction triggering of sand defined based on large R_u values (~100%) and/or large shear strains (e.g., Andrus and Stokoe 2000; Baxter et al. 2008).

4.6 Threshold Shear Strain for Cyclic Pore Water Pressure Generation

The threshold shear strain for cyclically induced pore water pressure (γ_{tvp}) (Dobry et al. 1982) is defined as the shear strain below which no noticeable permanent pore pressure is developed with an increasing number of cycles. Dobry and Abdoun (2015) stated that research using lab and field tests show that γ_{tvp} is a robust soil property for sands that is mostly independent of the number of loading cycles, sand type, nonplastic fines content, relative density, depositional method, and the effective confining pressure between 20 kPa to 200 kPa. Vucetic (1994) showed that γ_{tvp} slightly increases with PI for cohesive materials. His proposed range was further confirmed by Hsu and Vucetic (2006) and was slightly updated by Mortezaie and Vucetic (2016) based on data from two reconstituted clay soils. In Figure 12, the γ_{tvp} extracted from field shaking tests (Project O_24) using truck-mounted shakers are plotted against PI. The results for R_u versus shear strains (γ_c) from field cyclic tests are presented in detail in Stokoe et al. (2020) and Preciado et al. (2021)

and are included in Appendix C for completeness. For comparison, data from reconstituted clay soils by Mortezaie and Vucetic (2016) and natural intact alluvial plastic silt by Jana and Stuedlein (2021) are also plotted in Figure 12. The recommended range by Mortezaie and Vucetic (2016) reasonably envelops the data points from this study and other studies. Dobry and Abdoun (2015) reported that overconsolidation of sand increases γ_{tvp}. While the field shaking data in this study appear to confirm that such trends may also exist for silts, more data is required to reliably investigate this behavior. As a practical approach, it appears reasonable to continue using the range proposed by Mortezaie and Vucetic (2016) in engineering applications.

4.7 Predictive Equations for V&D Model Parameters for Silts

The relationships between V&D model parameters and other soil properties shown in previous plots were used to develop a set of predictive equations to estimate model parameters (i.e., γ_{tvp}, F, s, and P) as a function of PI, FC, and OCR for silt-rich soils. Note that these relationships are developed for low plasticity silts that classify as ML, CL or CL-ML based on the USCS classification system. The range of applicability of these equations include fine-grained soils with FC ranging from 50% to 100%, silt content ranging from 47% to 81%, PI ranging from NP to 16, and OCR ranging from 1 to 2.5. The proposed equations provide an improved means to select model parameters for silts compared to currently available data that is mostly obtained from sands. A useful compilation of available data can be found in the current DEEPSOIL User Manual (Hashash 2020) and the D-MOD2000 User Manual (Matasović and Ordonez 2011). The proposed equations provide insights on clear differences between sands and silty sands (FC<50%) and silts (FC>50%), and the important effects of OCR on the cyclic response of silts. However, some variations in responses could not be explained. These variations are likely due to inherent variability in tests performed on natural intact soils. Future test programs may further investigate this variability. Therefore, the equations provided below are recommended for the sake of bracketing likely ranges of parameters used in preliminary analyses. It is recommended that cyclic tests are performed as part of the project scope when the estimated pore pressures and cyclic softening of soils have a significant influence on design and associated risks.

The proposed relationships for V&D model parameters are listed below:

$$\gamma_{tvp}[\%] = 0.01 + PI/900 \quad (3)$$

(based on average of the recommended range by Mortezaie and Vucetic 2016)

$$P = 1.0 \times OCR^{-0.23} \quad (4)$$

$$F_{NC} = 0.7 \text{ (mean value for NC silt)} \quad (5a)$$

$$F_{OC} = F_{NC} \times OCR^{-2.5} \quad (5b)$$

$$s_{NC} = (1 + FC)^{0.1252} \text{ (the relationship proposed by Carlton 2014)} \quad (6a)$$

$$s_{OC} = s_{NC} \times OCR^{0.5} \quad (6b)$$

The accuracy of the proposed predictive equations for V&D model parameters for silts is evaluated by comparing the predicted and measured R_u values at the same shear strain and number of the loading cycle. In Figure 13a, the measured R_u values are compared to R_u values predicted using the V&D model when the model parameters are calculated using the proposed relationships in this study (Equations (3) to (6)). The R_u values plotted in this figure correspond to 35 strain-controlled CDSS tests with shear strains ranging from 0.07% to 2% and number of loading cycles ranging from 1 to 60. The 1:1, 1:2 and 2:1 lines are plotted for reference. The plotted data points are binned into three categories based on their PI to evaluate the potential influence of soil plasticity. R_u values smaller than 0.4 are, on average, underpredicted by the model; R_u values greater than 0.4 are generally overpredicted, but are bounded by the 1:2 and 2:1 lines. The model predictions seem to be slightly more accurate for low plasticity silts with PI<7. The scatter in the data is due to two sources of uncertainty: (a) the robustness of the proposed predictive equations in estimating the V&D model parameters, and (b) possible limitations in the applicability of the V&D model, which was originally developed for sand, to the fine-grained low-plasticity silts (FC≥50% and PI ranging from NP to 16) evaluated in this investigation. To differentiate the sources of uncertainty additional comparisons are made between measured and predicted R_u values, using V&D model parameters that are specifically calibrated for each set of lab data (reported in Table 2); these comparisons are shown in Figure 13b. The model is shown to reasonably predict R_u values larger than 0.4. This is expected, considering that the calibration procedure favored test data at larger shear strains and R_u values. This figure demonstrates that the V&D sand model can be effectively applied to fine-grained silts with PI ranging between NP to 16 if calibrated to lab data. The reduction in scatter from Fig. 13a to Fig. 13b highlights the benefit of performing cyclic lab tests to reduce uncertainty.

5 CONCLUDING REMARKS

A series of cyclic shear tests that includes 35 strain-controlled CDSS tests and field shaking tests on low-plastic silts from six different soils were used in this study to (a) evaluate the variation of cyclically induced excess pore pressures with various soil index properties and stress histories, and (b) provide calibrated Vucetic and Dobry (1986) model parameters for these tests. The focus in this study was on fine-grained, silt-rich soils with fines content (FC) ranging from 54% to 100%, silt content ranging from 47% to 83%, and plasticity index (PI) ranging from NP to 16. The evaluation of data in this study provided insights on differences between clean sands and silty sands (FC<50%) and fine-grained silts (FC>50%). The important effects of stress history and overconsolidation on the cyclic response of silts are listed below:

- R_u values in silts decrease with increasing FC, silt content, and PI and increase with increasing interfine void ratio. These trends were more obvious for tests performed at a cyclic shear strain of 0.1%, but were also observed in tests performed at larger cyclic strains (up to 2%).
- R_u values for OC silts with OCR ranging between 1.5 to 3 were found to be significantly smaller than those of NC soils with OCR = 1 for cyclic shear strains between 0.1% and 2%.
- The threshold shear strains for pore pressure generation (γ_{tvp}) were calculated from field shaking tests on silts with PI = 13 and OCR from 2.1 to 3. The values were found to be

enveloped by the range proposed by Mortezaie and Vucetic (2016), affirming that the threshold shear strain is a fundamental soil property.

- The calibrated V&D model parameters for silts were found to be significantly different from those reported in the literature for sands. The *F* parameter for NC silts (FC>50%) ranged from 0.3 to 1.1 with a mean value of 0.7, while the *F* parameter for sand (FC<50%) reported in the literature ranged from 0.7 to 10.9 with a mean value of 2.2.
- The calibrated V&D model parameters were significantly affected by OCR. The *F* and *P* parameters were found to decrease with OCR, while the *s* parameter increased with OCR.
- A set of predictive equations were developed to calculate V&D model parameters for low-plastic silts (FC>50% and PI between NP and 16) based on data in this study. The predicted and measured R_u values were generally bounded with 1:2 and 2:1 ratios.
- It was shown that performing strain-controlled cyclic shear tests on silts reduces the uncertainty in calibrating V&D models for design applications.

6 ACKNOWLEDGEMENTS

The authors thank the many individuals and organizations that provided data and support for this study: Jan Six (formerly with the Oregon Department of Transportation), Tony Allen (Washington State Department of Transportation), Scott Schlechter, Jason Bock, and Jack Gordon (GRI Inc.), Don Anderson and Nason McCullough (Jacobs), Park Piao, Sam Sideras, Bill Perkins, and Bob Mitchell (Shannon & Wilson), and Professor Kenneth Stokoe (University of Texas at Austin.) Support for field shaking was provided by Grant No. CMMI-1935670 from the National Science Foundation.

7 REFERENCES

Anderson, D. G., Shin, S., & Kramer, S. L. (2011). Nonlinear, Effective-Stress Ground Motion Response Analyses Following AASHTO Specifications for Load and Resistance Factor Design Seismic Bridge Design. Transp Res Rec;2251:144–54. https://doi.org/10.3141/2251-15

Andrus, R. D., & Stokoe II, K. H. (2000). Liquefaction resistance of soils from shear-wave velocity. J Geotech Geoenviron Eng;126:1015–25. https://doi.org/10.1061/(ASCE)1090-0241(2000)126:11(1015)

Armstrong, R. J., & Malvick, E. J. (2016). Practical considerations in the use of liquefaction susceptibility criteria. Earthq Spectra:32:1941–50. https://doi.org/10.1193/071114EQS100R

Baxter, C. D., Bradshaw, A. S., Green, R. A., & Wang, J. H. (2008). Correlation between cyclic resistance and shear-wave velocity for providence silts. J Geotech Geoenviron Eng;134:37–46. https://doi.org/10.1061/(ASCE)1090-0241(2008)134:1(37)

Bray, J. D., & Sancio, R. B. (2006). Assessment of the liquefaction susceptibility of fine-grained soils. J Geotech Geoenviron Eng; 132:1165–77. https://doi.org/10.1061/(ASCE)1090-0241(2006)132:9(1165)

Carlton, B. (2014). An improved description of the seismic response of sites with high plasticity soils, organic clays, and deep soft soil deposits. PhD Dissertation. University of California, Berkeley

CH2M Hill (2008). I-5 Tacoma/Pierce County HOV Program Portland Avenue to Port of Tacoma Project Puyallup River Bridge (BR 5/456) – Site-Specific Seismic Ground Response Analysis using DMOD2000. Prepared for Washington State Department of Transportation Headquarter Geotechnical, April 29, 2008.

CH2M Hill (2009). WSDOT General Mark W. Clark Memorial Bridge (532/2) Seismic Response Study XL-2770. Prepared for Washington Department of Transportation Headquarters Geotechnical Branch, February 2009.

Dahl, K. R., DeJong, J. T., Boulanger, R. W., Pyke, R., and Wahl, D. (2014). Characterization of an alluvial silt and clay deposit for monotonic, cyclic and post-cyclic behavior. Can Geotech J;51:432 –40. https://doi.org/10.1139/cgj-2013-0057

Dahl, K., Boulanger, R. W., & DeJong, J. T. (2018). Trends in experimental data of intermediate soils for evaluating dynamic strength. In: Proceedings of the 11th US National Conference on Earthquake Engineering. Los Angeles, Calif.: Earthquake Engineering Research Institute, June.

DeJong, J. T., Krage, C. P., Albin, B. M., & DeGroot, D. J. (2018). Work-based framework for sample quality evaluation of low plasticity soils. J. Geotech Geoenviron Eng; *144*(10), 04018074.

Dobry, R., Ladd, R. S., Yokel, F. Y., Chung, R. M., & Powell, D. (1982). Prediction of pore water pressure buildup and liquefaction of sands during earthquakes by the cyclic strain method (Vol. 138, p. 150). Gaithersburg, MD: National Bureau of Standards.

Dobry, R., Pierce, W. G., Dyvik, R., Thomas, G. E., & Ladd, R. S. (1985). Pore pressure model for cyclic straining of sand. Troy, New York: Rensselaer Polytechnic Institute.

Dobry, R. and Vucetic, M., (1987). State-of-the-Art Report: Dynamic Properties and Response of Soft Clay Deposits. Proceedings of the International Symposium on Geotechnical Engineering of Soft Soils, Mexico City, Editors: Mendoza, M.J. and Montanez, L, Publisher: Sociedad Mexicana de Mecanica de Suelos, Mexico City, August, Vol. 2, pp. 51-87

Dobry, R., & Abdoun, T. (2015). Cyclic shear strain needed for liquefaction triggering and assessment of overburden pressure factor k σ. J Geotech Geoenviron Eng;141:04015047. https://doi.org/10.1061/(ASCE)GT.1943-5606.0001342

Green, R.A., Mitchell, J.K. and Polito, C.P. (2000). An Energy-Based Pore Pressure Generation Model for Cohesionless Soils, Proceedings: John Booker Memorial Symposium, Melbourne, Australia, November 16-17, 2000.

GRI (2012). Cyclic Testing Data Report ODOT OR!8: Newberg-Dundee Bypass. Prepared for ODOT Region 2 Bridge/Geo/Hydro Unit, October 3, 2012.

Hashash, Y.M.A., Musgrove, M.I., Harmon, J.A., Ilhan, O., Xing, G., Numanoglu, O., Groholski, D.R., Phillips, C.A., and Park, D. (2020). DEEPSOIL 7.0, User Manual. Urbana, IL, Board of Trustees of University of Illinois at Urbana-Champaign.

Hazirbaba, K., & Rathje, E. M. (2009). Pore pressure generation of silty sands due to induced cyclic shear strains. J Geotech Geoenviron Eng;135:1892–1905. https://doi.org/10.1061/(ASCE)GT.1943-5606.0000147

Hsu, C. C., & Vucetic, M. (2006). Threshold shear strain for cyclic pore-water pressure in cohesive soils. J Geotech Geoenviron Eng;132:1325–35. https://doi.org/10.1061/(ASCE)1090-0241(2006)132:10(1325)

Idriss, I. M., & Boulanger, R. W. (2008). Soil liquefaction during earthquakes. 2nd Ed. Oakland, Calif.: Earthquake Engineering Research Institute.

Jana, A., & Stuedlein, A. W. (2021). Monotonic, Cyclic, and Postcyclic Responses of an Alluvial Plastic Silt Deposit. J Geotech Geoenviron Eng;147: 04020174. https://doi.org/ 10.1061/(ASCE)GT.1943-5606.0002462

Koester, J. P. (1994). The influence of fine type and content on cyclic resistance. In: Ground failures under seismic conditions (Geotech. Spec. Publ. No. 44). New York: American Society of Civil Engineers; 17–33.

Lunne, T., Berre, T., Andersen, K. H., Strandvik, S., & Sjursen, M. (2006). Effects of sample disturbance and consolidation procedures on measured shear strength of soft marine Norwegian clays. Canadian Geotechnical Journal, *43*(7), 726-750.

Matasović N. (1993). Seismic response of composite horizontally-layered soil deposits, Ph.D. Thesis, Los Angeles, Calif.: University of California, Los Angeles.

Matasović, N. and Vucetic M. (1993). Seismic Response of Composite Horizontally-Layered Soil Deposits, UCLA Research Report No. ENG-93-182, Civil Engineering Department, University of California, Los Angeles, CA, March, 452 p.

Matasovic, N. and Vucetic, M. (1995). Seismic Response of Soil Deposits Composed of Fully-Saturated Clay and Sand Layers, Proceedings of the 1st International Conference on Geotechnical Earthquake Engineering, Tokyo, Japan, Editor: Ishihara, K., Publisher: A.A. Balkema, Rotterdam/Brookfield, Vol. I, pp. 611-616. November.Matasović, N., & Ordonez, G. (2012). D-MOD2000–A computer program for seismic site response analysis of horizontally layered soil deposits, earthfill dams and solid waste landfills: User's manual. Lacey, Wash.: Geomotions, LLC. Available at http://www.geomotions.com/Download/D-MOD2000Manual.pdf

Matasović, N. and Vucetic, M. (1995). Generalized cyclic-degradation-pore-pressure generation model for clays. J Geotech Eng 121:33–42. https://doi.org/10.1061/(ASCE)0733-9410(1995)121:1(33)

McCullough, N. J., Hoffman, B., Takasumi, D. L., Anderson, D. G., & Dickenson, S. E. (2009). Seismic Site Response for an LNG Facility—Analyses and Lessons Learned. In TCLEE 2009: Lifeline Earthquake Engineering in a Multihazard Environment; pp. 1–12. https://doi.org/10.1061/41050(357)111

Mei, X., Olson, S.M. and Hashash, Y.M. (2018). Empirical porewater pressure generation model parameters in 1-D seismic site response analysis. Soil Dyn Earthq Eng 114:563–7. https://doi.org/10.1016/j.soildyn.2018.07.011

Mitchell, J. K., & Soga, K. (2005). Fundamentals of Soil Behavior. 3rd Ed. New York: John Wiley & Sons.

Mortezaie, A. R., & Vucetic, M. (2013). Effect of frequency and vertical stress on cyclic degradation and pore water pressure in clay in the NGI simple shear device. *Journal of Geotechnical and Geoenvironmental Engineering*, *139*(10), 1727-1737.

Mortezaie, A., & Vucetic, M. (2016). Threshold shear strains for cyclic degradation and cyclic pore water pressure generation in two clays. J Geotech Geoenviron Eng;142:04016007. https://doi.org/10.1061/(ASCE)GT.1943-5606.0001461

Mousavi, S., & Ghayoomi, M. (2021). Liquefaction mitigation of sands with nonplastic fines via microbial-induced partial saturation. J Geotech Geoenviron Eng;147:04020156. https://doi.org/10.1061/(ASCE)GT.1943-5606.0002444

Polito, C. P., & Martin II, J. R. (2001). Effects of nonplastic fines on the liquefaction resistance of sands. J Geotech Geoenviron Eng;127:408–15. https://doi.org/10.1061/(ASCE)1090-0241(2001)127:5(408)

Preciado, A. M., Sorenson, K., Khosravifar, A., Moug, D., Stokoe, K., Menq, F., & Zhang, B. (2021). Evaluating cyclic loading response of a low plasticity silt with laboratory and field cyclic loading tests. ASCE Lifelines 2021 Conference UCLA. Reston, Va.: American Society of Civil Engineers.

Shannon and Wilson, Inc. (2004). Seismic Ground Motion Study Report – SR99: Alaskan Way Viaduct and Seawall Replacement Project. Prepared for Washington State Department of Transportation Urban Corridors Office, October 2004.

Shen, C. K., Vrymoed, J. L., and Uyeno, C. K. (1977). The effects of fines on liquefaction of sands. In: Proceedings of the 9th International Conference on Soil Mechanics and Foundation Engineering, Vol. 2. Tokyo, Japan: Japanese Society of Soil Mechanics and Foundation Engineering; pp. 381–5.

Stokoe, K.H., Zhang, B., and Menq, F. (2020). Field Assessment of the Microbially Induced Desaturation (MID) Method to Mitigate Liquefaction in Silty Soils with Plasticity. GEotechncial Engineering Report GR20-04, Geotechnical Engineering Center, The University of Texas at Austin; 58 p.

Tan, T.S., Lee, F.H., Chong, P.T., and Tanaka, H. (2002). Effect of sampling disturbance on properties of Singapore clay. Journal of Geotechnical and Geoenvironmental Engineering, 128(11): 898-906.

Thevanayagam, S., Shenthan, T., Mohan, S., & Liang, J. (2002). Undrained fragility of clean sands, silty sands, and sandy silts. J Geotech Geoenviron Eng;128:849–59. https://doi.org/10.1061/(ASCE)1090-0241(2002)128:10(849)

Thevanayagam, S. (2007). Intergrain contact density indices for granular mixes—I: Framework. Earthq Eng Eng Vib;6:123. https://doi.org/10.1007/s11803-007-0705-7

Thilakaratne, V. and Vucetic, M. (1987). Class-A Prediction of Accelerations and Seismic Pore Pressures at the Owi Island Site during Oct. 4 1985 Earthquake in Tokyo Bay-Part I. Research Report, Civ. Eng. Dept., Potsdam, NY: Clarkson Univ.; 60 p.

Troncoso, J. H., and Verdugo, R. (1985). Silt content and dynamic behavior of tailing sands. Proceedings of the 12th International Conference on Soil Mechanics and Foundations Engineering; pp. 1311–14.

Vaid, Y. P. (1994). Liquefaction of silty soils. In: Prakas S, Dakoulas, P (Eds.) Ground failures under seismic conditions. Reston, Va.: ASCE; October, pp. 1–16

Vucetic, M. (1986). Pore Pressure Buildup and Liquefaction at Level Sandy Sites During Earthquakes (California, Japan). PhD dissertation. Troy, NY: Rensselaer Polytechnic Institute.

Vucetic M, Dobry R. (1986). Pore pressure build-up and liquefaction at level sandy sites during earthquakes, Research report CE-86-3. Troy, NY: Rensselaer Polytechnic Institute.

Vucetic, M., (1988). Normalized Behavior of Offshore Clay Under Uniform Cyclic Loading, Canadian Geotechnical Journal, Vol. 25, No. 1, pp. 33-41

Vucetic, M. and Dobry, R. (1988). Cyclic triaxial strain-controlled testing of liquefiable sands. In: RT Donaghe, RC Chaney, ML Silver (Eds.), Advanced triaxial testing of soil and rock. West Conshohocken, Pa.: ASTM International; https://doi.org/10.1520/STP977-EB

Vucetic, M. (1994). Cyclic threshold shear strains in soils. J Geotech Eng;120:2208–28. https://doi.org/10.1061/(ASCE)0733-9410(1994)120:12(2208)

Wijewickreme, D., Soysa, A., & Verma, P. (2019). Response of natural fine-grained soils for seismic design practice: A collection of research findings from British Columbia, Canada. Soil Dyn Earthq Eng 124, 280–96. https://doi.org/10.1016/j.soildyn.2018.04.053

Zapata-Medina, D.G., Finno, R.J., and Vega-Posada, C.A. (2014). “Stress history and sampling disturbance effects on monotonic and cyclic responses of overconsolidated Bootlegger Cove clays.” Canadian Geotechnical Journal, 51: 599-609.

Table 1. Cyclic shear tests used in this study

Proj. ID	Project / Location	Soils	Reference	Boring, Sample ID (Depth)	γ_c in Strain-controlled CDSS Tests (%)	Cyclic loading rate (Hz)	D60 / D10 (mm)	Sand / Silt / Clay (%)	FC (%)	PL / LL (PI)	USCS Class.	Natural water content (%)	Void ratio	Consol. Vert. stress (kPa) / Vert. effective stress prior to cyclic loading (kPa) / OCR	V_s (m/s)
O_15	ODOT SR 18 Newberg-Dundee By-Pass / Oregon	Willamette Silt / Missoula Flood FF	GRI (2012)	B86, U3 (4.6 m)	0.1, 0.4, 1.6	0.1	0.009 / 0.001	0 / 64 / 36	100	23 / 39 (16)	CL	37.9 - 43.1	1.02 - 1.16	240 / 240 / 1	243
				B153, U5 (9.1 m)	0.1, 0.4, 1.6	0.1	0.011 / 0.0005	1 / 79 / 20	99	21 / 30 (9)	CL	32.4 - 36.3	0.88 - 0.98	240 / 240 / 1	350
				B153, U4 (6.1 m)	0.1, 0.4, 1.6	0.1	0.085 / 0.01	46 / 49 / 5	54	28 / 33 (5)	ML	33.3 - 35.3	0.90 - 0.95	360 / 240 / 1.5	497
				B86, U4 (6.1 m)	0.1, 0.4, 2	0.1	0.018 / 0.0015	3 / 77 / 20	97	24 / 30 (6)	ML	32.8 - 35	0.89 - 0.96	600 / 240 / 2.5	802
W_01	WS SR-532, General Mark W. Clark Bridge / Stanwood, WA	Tidal Silt / Marine Estuarine	Anderson et al. (2011); CH2M Hill (2009)	GMWC-1C-08, ST-2 (10.4 m)	0.1, 0.7	0.1	0.075 / 0.007	39 / 53 / 8	61	23 / 31 (8)	ML	32.3	0.88	144 / 144 / 1 158 / 158 / 1	256 – 282
				GMWC-1A-08, ST-5 (26.5 m)	0.1, 0.7	0.1	0.015 / 0.001	13 / 63 / 24	87	22 / 32 (10)	ML	33	0.71	321 / 321 / 1 350 / 350 / 1	572 – 623
				GMWC-1A-08, ST-1 (15.2 m)	0.1, 0.4, 1.6	0.1	0.35 / 0.15	99 / 1 / 0	1	NA	SP	23.8	0.75	187 / 187 / 1 201 / 201 / 1 215 / 215 / 1	271
				GMWC-1A-08, ST-4 (24.4 m)	0.1, 0.4, 1.6	0.1	0.112 / 0.04	68 / 31 / 1	32	NA	SM	26.5	0.7	297 / 297 / 1 321 / 321 / 1 350 / 350 / 1	263
O_01	Proposed Oregon LNG Facility / Warrenton, OR	Columbia River Silt	McCullough et al. (2009)	BH-6, 40-ST (75.6 m)	3 stress-controlled CDSS *	0.1	NA	1 / 81 / 18	99	25 / 37 (12)	ML	37.3	0.97	800 / 800 / 1	331
				BH-10, 26-ST (40 m)	3 stress-controlled CDSS *	0.1	NA	27 / 67 / 6	73	26 / 36 (10)	ML	33.4 - 34.1	0.89 - 0.91	400 / 400 / 1	311
W_03	WS SR-99, Alaskan Way Viaduct / Seattle, WA	Tidal Silt / Marine Estuarine	Shannon and Wilson (2004)	SDC-001, S-18 (21.6 m)	0.29	0.01 to 0.05	0.06 / 0.004	28 / 66 / 6	72	NP	ML	38.4	0.879	200 / 200 / 1	NA
				SDC-001, S-24 (26.2 m)	0.1	0.01 to 0.1	0.1 / 0.006	46 / 48 / 6	54	23 / 28 (5)	ML	35.6	0.825	223 / 223 / 1	NA
				SDC-001, S-24 (26.2 m)	0.075	0.05 to 0.1	0.06 / 0.002	29 / 66 / 5	71	NP	ML	35.2	0.781	400 / 400 / 1	NA
				SDC-002, S-19 (15.8 m)	0.165	0.05 to 0.1	0.065 / 0.004	37 / 60 / 3	63	NP	ML	38.7	0.957	150 / 150 / 1	NA
W_08	I-5 Puyallup River Bridge / Tacoma, WA	Fluvial Silt	CH2M Hill (2008)	5/456-H-19vwp, ST-4 (4.9 m)	0.1, 0.4, 1.6	0.1	0.07 / 0.003	39 / 48 / 13	61	33 / 43 (10)	ML	42.6	1.14	52 / 52 / 1	117
				WR-12-H-1p-08, ST-16 (20.4 m)	0.1, 0.4, 1.6	0.1	0.09 / 0.009	46 / 47 / 7	54	NP	ML	24.8	0.66	220 / 220 / 1	212
				WR-12-H-1p-08, ST-20 (25.6 m)	0.1, 0.4, 1.6	0.1	0.055 / 0.004	23 / 66 / 11	77	21 / 27 (6)	CL-ML	31.7	0.82	480 / 480 / 1	250
O_24	Sunderland / Portland, OR	Columbia River Silt	Stokoe et al. (2020); Preciado et al. (2021) **	TREX-1P (1.55 m)	0.001 to 0.142	10	NA	10 / 70 / 20	90	25 / 38 (13)	ML	39.5	1.15	92 / 44 / 2.1	92
				TREX-2P (1.75 m)	0.001 to 0.246	10	NA	10 / 70 / 20	90	25 / 38 (13)	ML	39.5	1.15	96 / 43 / 2.2	92
				TREX-SC7 (2.55 m)	0.001 to 0.185	10	0.015 / 0.001	10 / 70 / 20	90	25 / 38 (13)	ML	39.5	1.15	128 / 42 / 3	116
				TREX-4P (4.55 m)	0.004 to 0.031	10	0.017 / 0.001	5 / 75 / 20	95	31 / 48 (17)	ML	49.5	1.275	110 / 52 / 2.1	100

* Stress-controlled test data reduced to excess pore pressures at average strains by McCullough et al. (2009) based on procedures by Matasović and Vucetic (1993)

** Field shaking. Preconsolidation stress determined from oedometer test, in-situ vertical effective stress includes the weight of truck-mounted shakers (T-Rex)

Table 2. Sample quality evaluation

Project	Boring, Sample ID	$\Delta e/e_o$ sample quality designation[a]	C_r/C_c sample quality rating[b]	$V_{s,lab}/V_{s,in\ situ}$	Gamma image taken to select intact sample?
O_15:	B86, U3	(1)	High	NA	No
	B153, U5	(2)	High	NA	
	B153, U4	(2)	High	NA	
	B86, U4	(1)	High	NA	
W_01	GMWC-1C-08, ST-2	(2)[c]	NA	1.2	Yes – specimens prepared from intact sections
	GMWC-1A-08, ST-5	(2)[c]	NA	0.8	
	GMWC-1A-08, ST-1	(1)[c]	NA	1.2	
	GMWC-1A-08, ST-4	(2)[c]	NA	1.1	
O_01	BH-6, 40-ST	(4)[c]	NA	1.0	Yes – images indicate some fracturing throughout samples
	BH-10, 26-ST	(3)[c]	NA	1.1	
W_03	SDC-001, S-18	NA	NA	NA	No
	SDC-001, S-24	NA	NA	NA	
	SDC-001, S-24	NA	NA	NA	
	SDC-002, S-19	NA	NA	NA	
W_08	5/456-H-19vwp, ST-4	(2)	NA	0.9	Yes – specimens prepared from intact section
	WR-12-H-1p-08, ST-16	(2)	NA	1.1	
	WR-12-H-1p-08, ST-20	NA	NA	0.9	

[a]Lunne et al (2006): (1) = very good to excellent, (2) = good to fair, (3) = poor, (4) = very poor
[b]DeJong et al. (2018): sample quality ratings are High, Moderate, and Low
[c]assessed from change in void ratio during reconsolidation to $1.2\sigma'_{vo}$

Table 3. Calibrated V&D parameters

Project / Soil Unit	Boring, Sample ID (USCS), Soil Properties	f	P	γ_{tvp}	F	s
O_15: SR18 Newberg-Dundee (Willamette Silt / Missoula Flood FF)	B86, U3 (CL) PI = 16, FC = 100%, OCR = 1, V_s = 243 m/s	1	0.94	0.03	1.10	1.90
	B153, U5 (CL), PI = 9, FC = 99%, OCR = 1, V_s = 350 m/s	1	0.95	0.020	1.00	2.00
	B153, U4 (ML), PI = 5, FC = 54%, OCR = 1.5, V_s = 497 m/s	1	0.94	0.015	0.56	2.20
	B86, U4 (ML), PI = 6, FC = 97%, OCR = 2.5, V_s = 802 m/s	1	0.80	0.020	0.04	3.10
W_01: WS SR-532, General Mark W. Clark Bridge (Estuarine/Tidal Silt)	1C-08, ST-2 (ML), PI = 8, FC = 61%, OCR = 1, V_s = 256–282 m/s	1	1	0.020	1.05	1.50
	1A-08, ST-5 (ML), PI = 10, FC = 87%, OCR = 1, V_s = 572–623 m/s	1	1	0.020	0.90	1.60
	1A-08, ST-1 (SP), PI = NP, FC = 1%, OCR = 1, V_s = 271 m/s	1	1	0.015	2.6	1.5
	1A-08, ST-4 (SM), PI = NP, FC = 32%, OCR = 1, V_s = 263 m/s	1	1	0.015	1.4	1.6
O_01: Warrenton, OR (Columbia River Silt)	BH-6, 40-ST (ML), PI = 10 to 12, FC = 73% to 99%, OCR = 1, V_s = 311–331 m/s	1	1.00	0.060	0.493	1.761
W_03: WS SR-99, Alaskan Way Viaduct (Estuarine/Tidal Silt)	SDC-001, S-18, S-24, SDC-002, S-19 (ML), PI = NP to 5, FC = 54% to 72%, OCR = 1	1	1.00	0.015	0.80	1.60
W_08: I-5/Puyallup River Bridge (Fluvial Silt)	H-19vwp, ST-4 (ML)), PI = 10, FC = 61%, OCR = 1, V_s = 117 m/s	1	0.80	0.020	0.30	1.30
	H-1p-08, ST-16 (ML), PI = NP, FC = 54%, OCR = 1, V_s = 212 m/s	1	1.00	0.015	0.50	1.30
	H-1p-08, ST-20 (CL-ML), PI = 6, FC = 77%, OCR = 1, V_s = 250 m/s	1	1.00	0.020	0.30	1.60
W_04: Alaskan Way Viaduct (Estuarine/Tidal Silt)	Reconstituted (ML), OCR = 1.2	1	1	0.015	0.54	2
O_24: Columbia River Silt, Portland, OR (Columbia River Silt)	Field shaking (ML), PI = 13, FC = 90%, OCR = 2.1-3, V_s = 92–116 m/s	1	0.81*	0.015	0.02	3
		1	0.81*	0.015	0.2	2.5

* Shear strains from field shaking tests were not large enough to constrain model paramter *P*. Instead, paramter *P* was estimated for these tests using the predictive equation shown in Figure 10c.

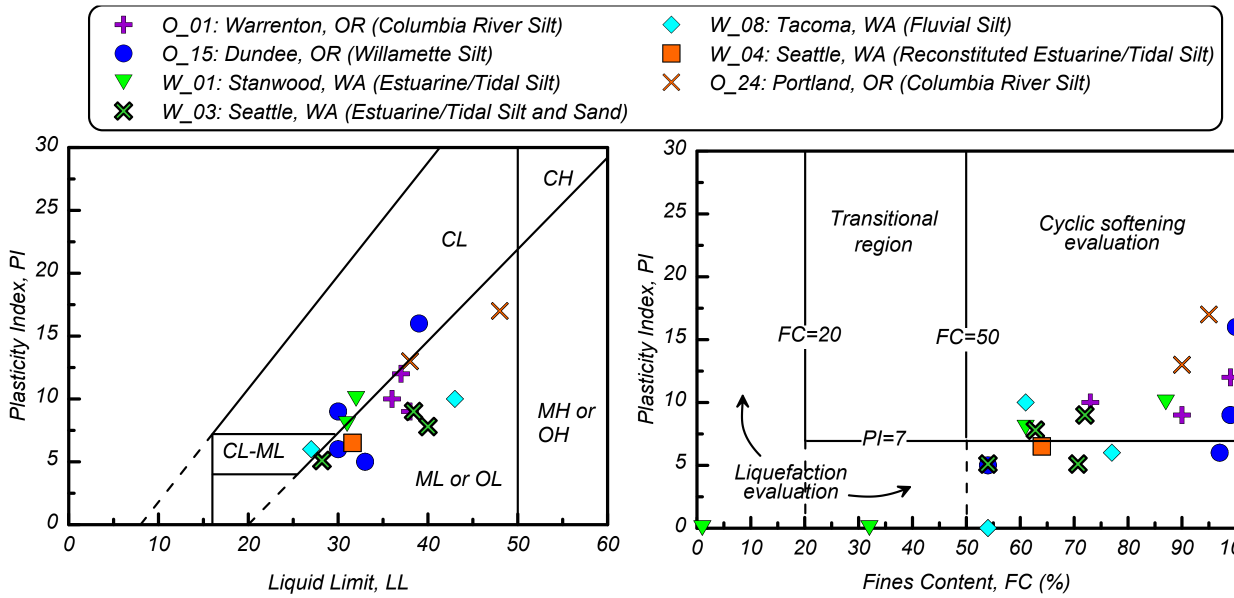

Figure 1: Atterberg limits and fines contents of the soils used in this database and the screening liquefaction and cyclic softening criteria by Idriss and Boulanger (2008) using the illustration by Armstrong and Malvick (2015).

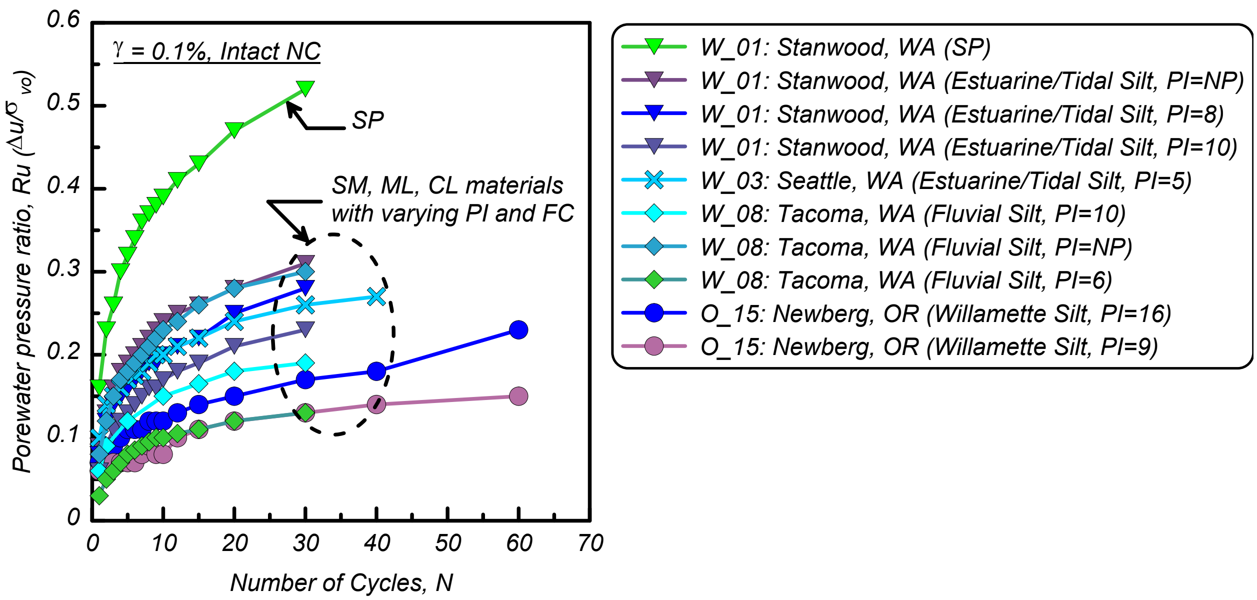

Figure 2: Variation of cyclically induced porewater pressure ratio with the number of uniform loading cycles at a constant cyclic shear strain of γ_c = 0.1% for intact, natural normally consolidated (NC) specimens with different FC (0% to 100%) and PI (NP to 16).

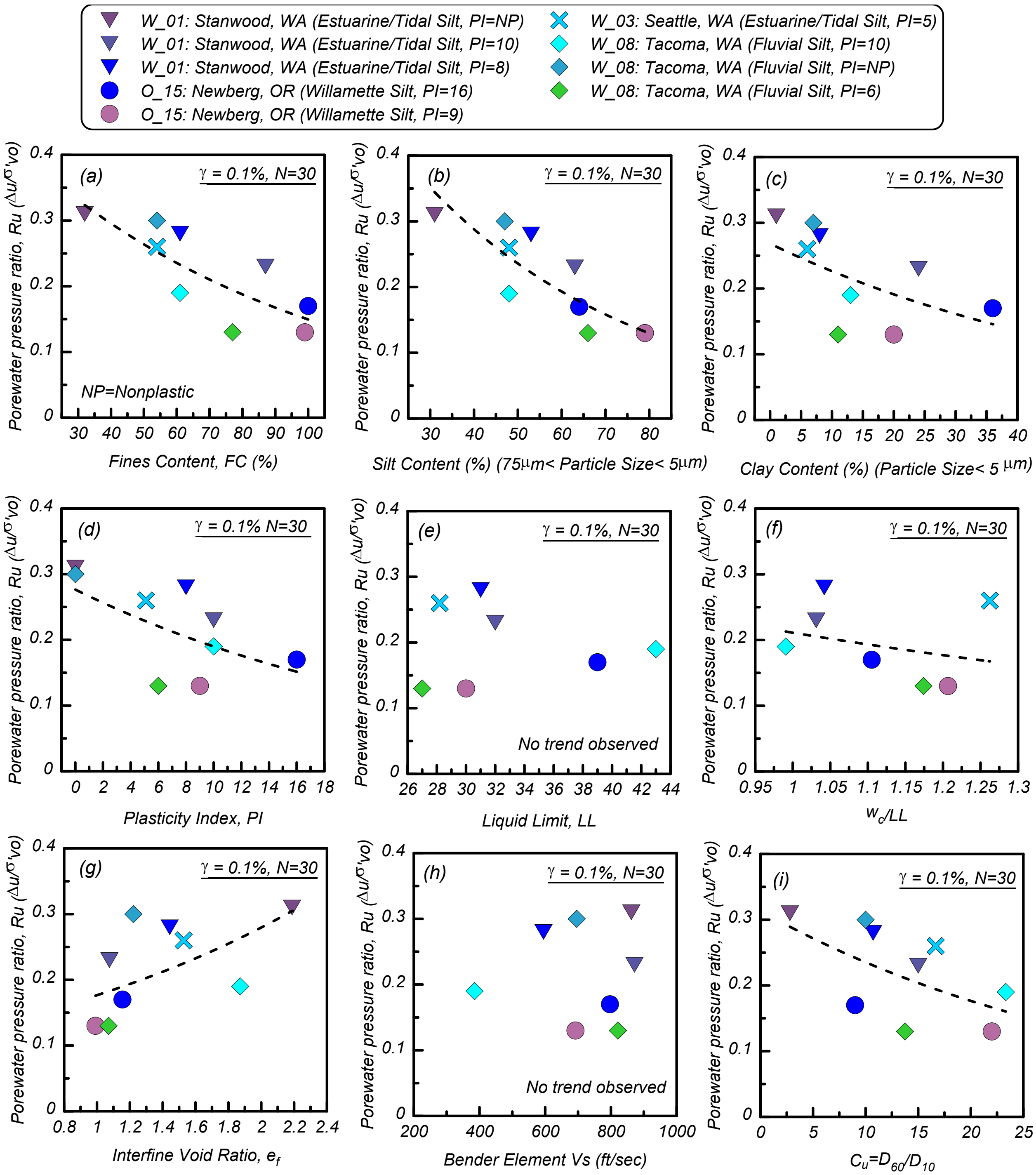

Figure 3: Variation of cyclically-induced porewater pressure ratio after 30 uniform loading cycles at a constant cyclic shear strain of γ_c = 0.1% with (a) fines content, (b) silt content, (c) clay content, (d) plasticity index (PI), (e) liquid limit (LL), (f) water content to liquid limit ratio, (g) interfine void ratio (e_f), (h) bender element shear velocity, and (i) coefficient of uniformity (C_u) for intact, natural normally consolidated (NC) specimens.

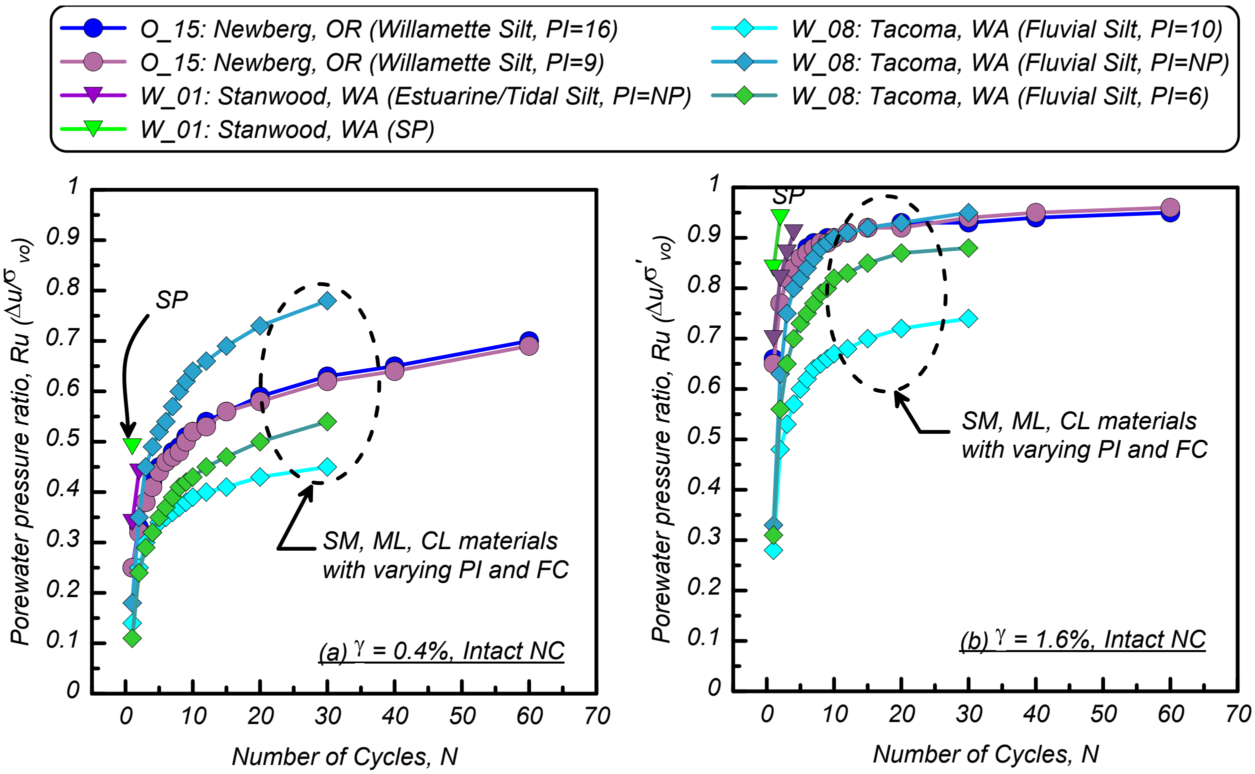

Figure 4: Variation of cyclically induced porewater pressure ratio with number of uniform loading cycles at a constant cyclic shear strain of (a) γ_c = 0.4% and (b) γ_c = 1.6% for intact, natural NC specimens with different FC (0% to 100%) and PI (NP to 16) values.

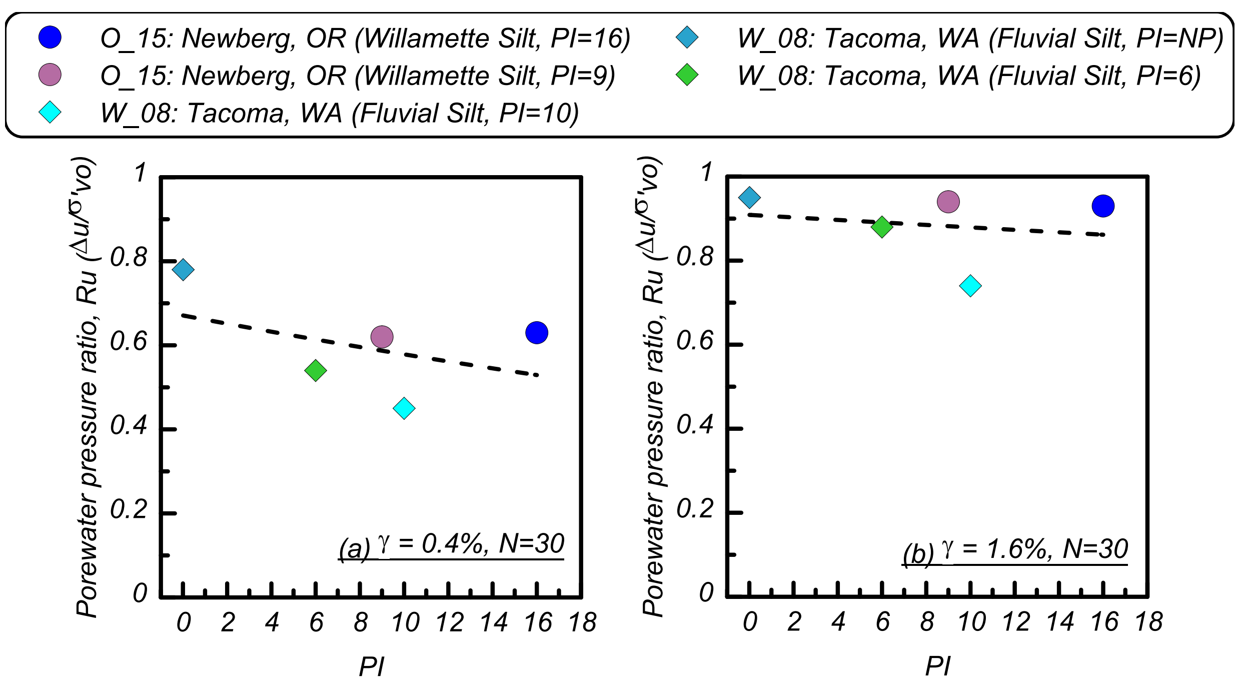

Figure 5: Variation of cyclically induced porewater pressure ratio after 30 uniform loading cycles at a constant cyclic shear strain of (a) γ_c = 0.4% and (b) γ_c = 1.6% with plasticity index for intact, natural, normally consolidated specimens.

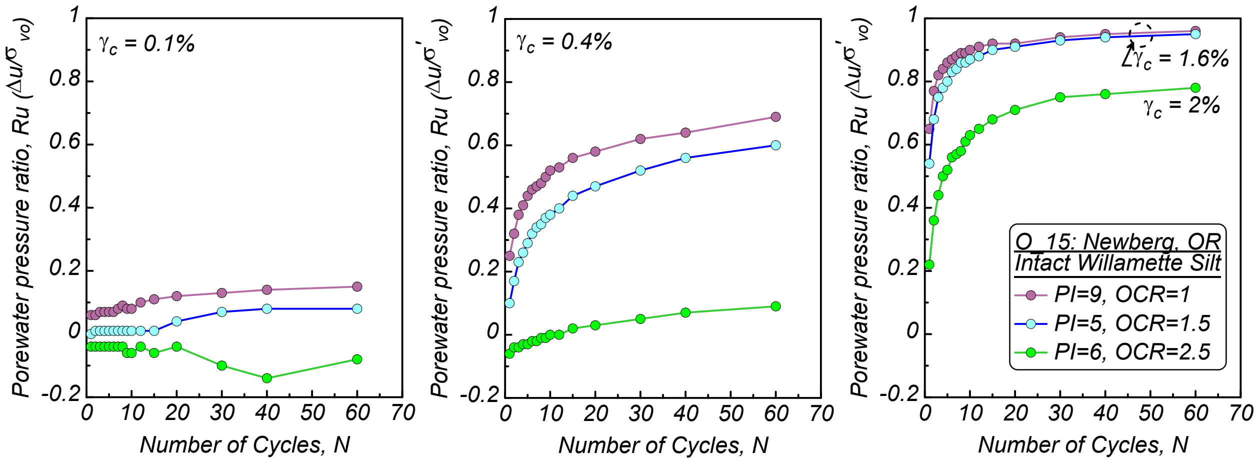

Figure 6: Variation of cyclically-induced porewater pressure ratio with number of uniform loading cycles at a constant cyclic shear strain of (a) γ_c = 0.1% and (b) γ_c = 0.4% and (c) γ_c = 1.6%–2% for intact, natural NC and OC specimens from Willamette Silt with PIs ranging from 5 to 9 (Project O_15).

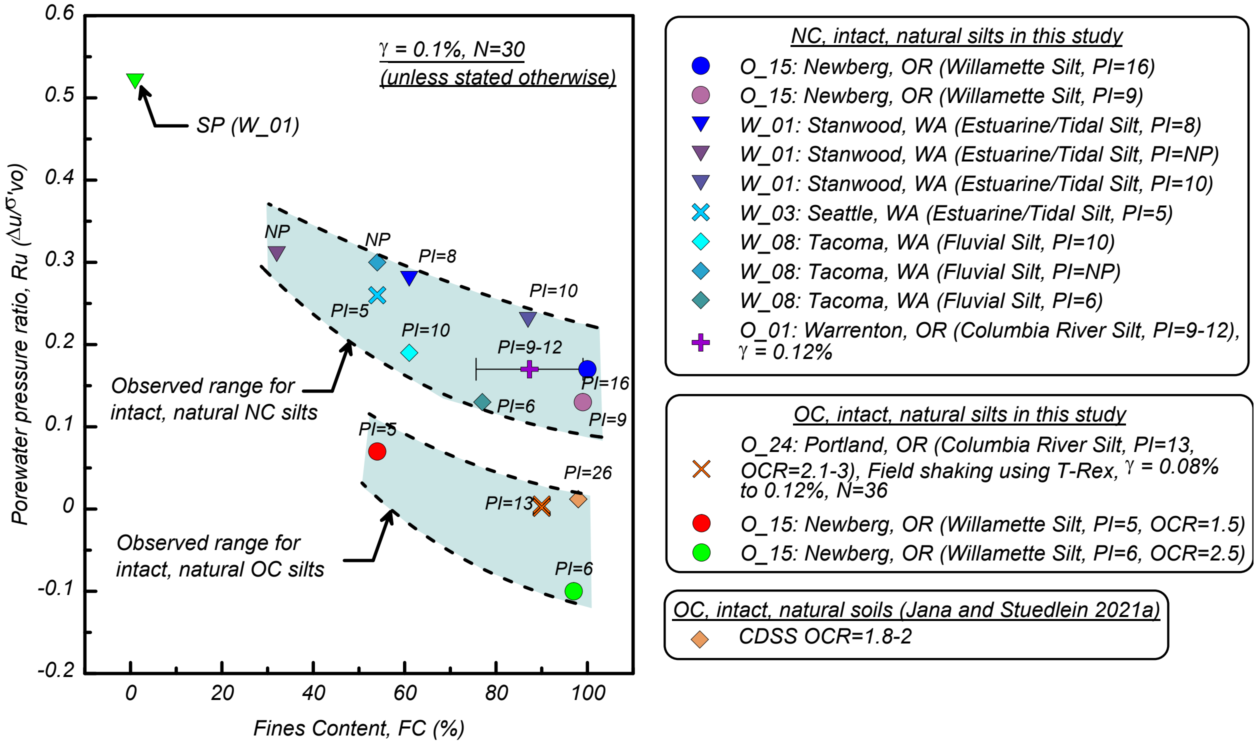

Figure 7: Effect of overconsolidation ratio (OCR) on cyclically-induced porewater pressure ratios at constant cyclic shear strain of γ_c = 0.1% for intact, natural specimens.

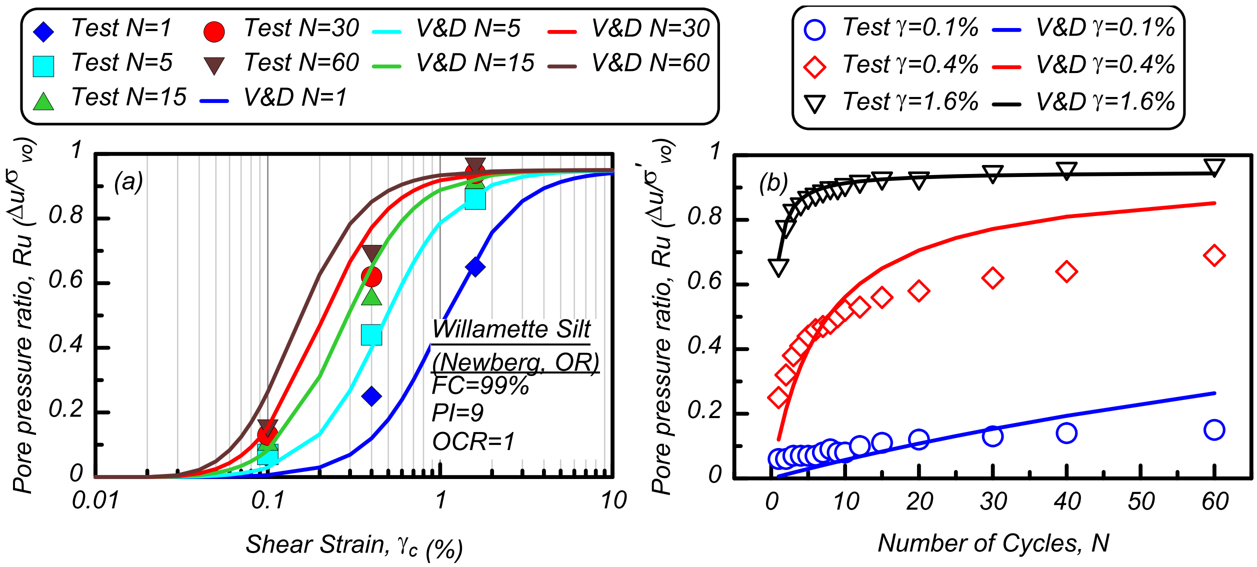

Figure 8: Comparison of measured and predicted R_u from CDSS tests and calibrated V&D model for intact, natural NC samples from Willamette Silt, FC=99%, PI=9 (Project O_15).

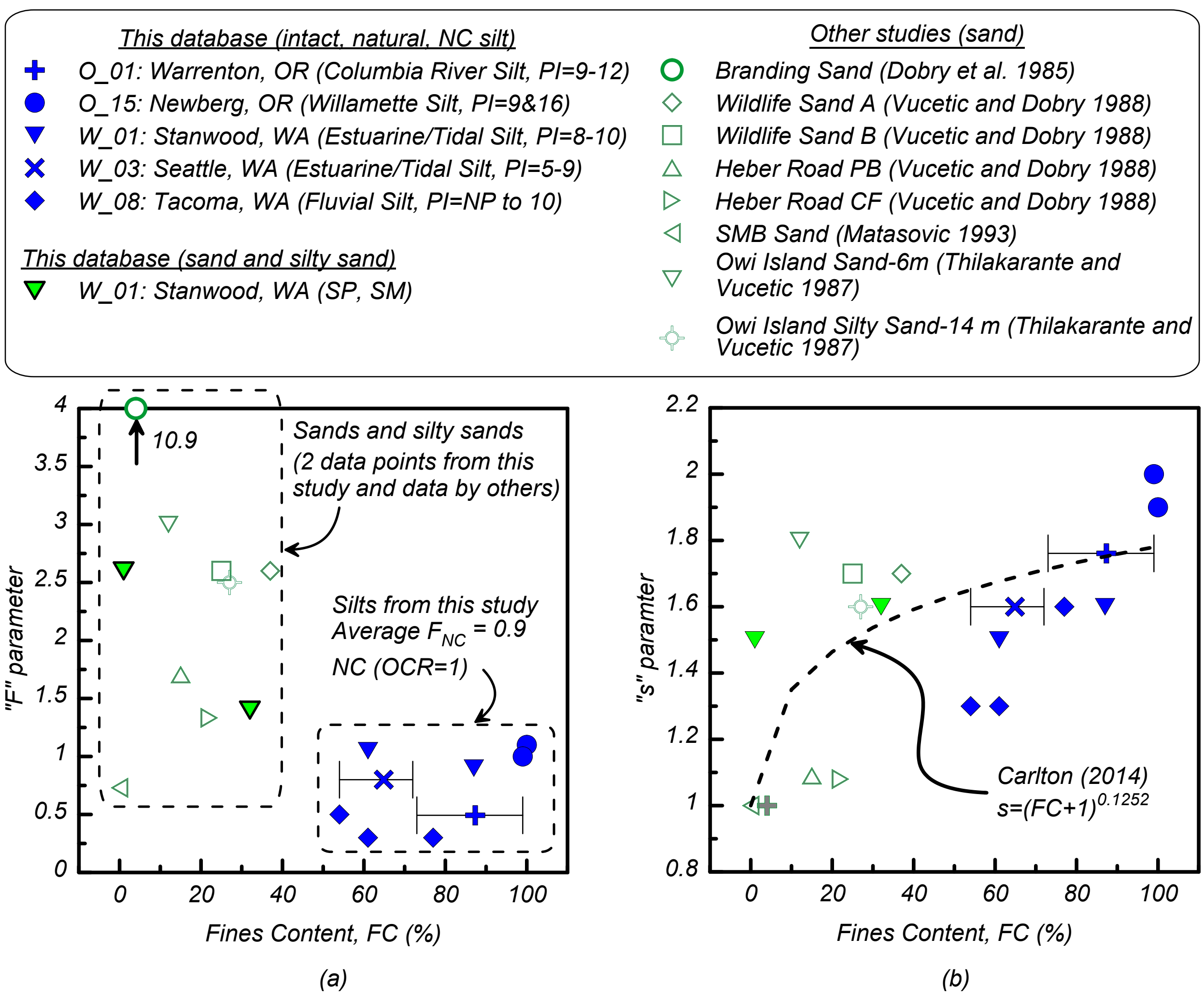

Figure 9: Variation in (a) Parameter *F* and (b) Parameter *s* in the V&D model with FC.

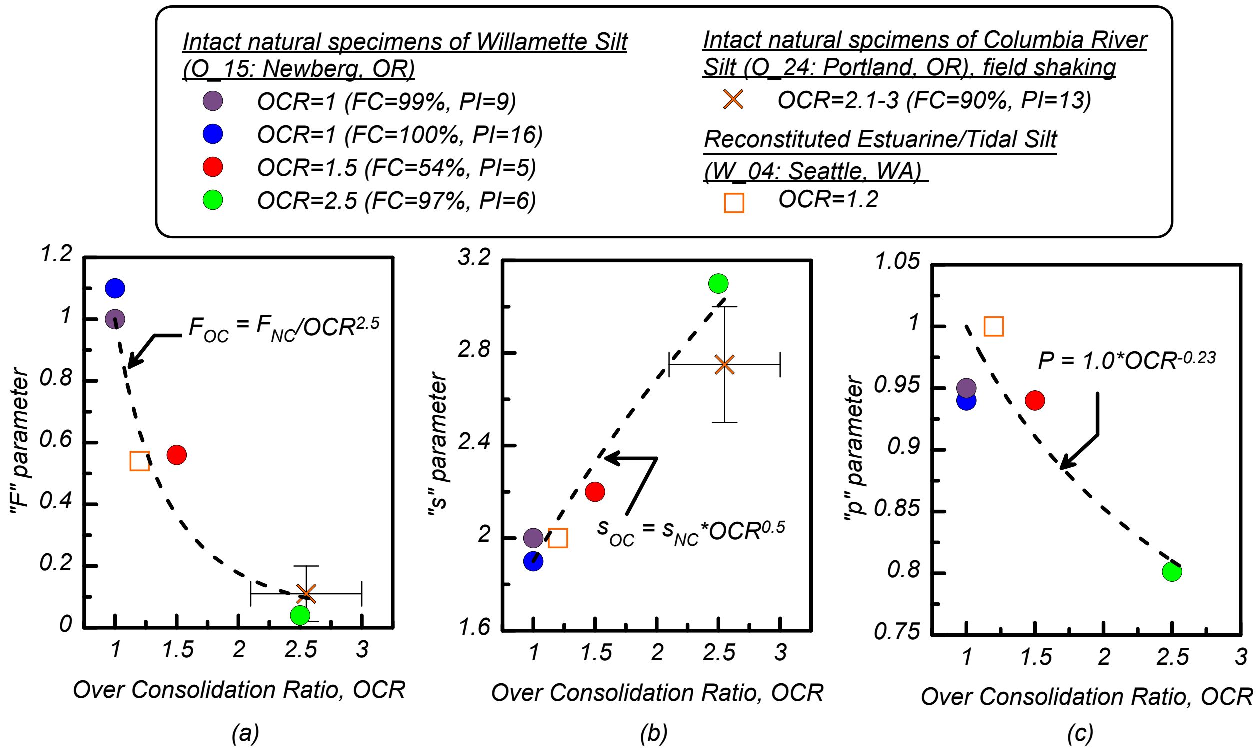

Figure 10: Effects of overconsolidation ratio (OCR) on (a) Parameter *F*, (b) Parameter *s*, and (c) Parameter *P* in the Vucetic and Dobry model.

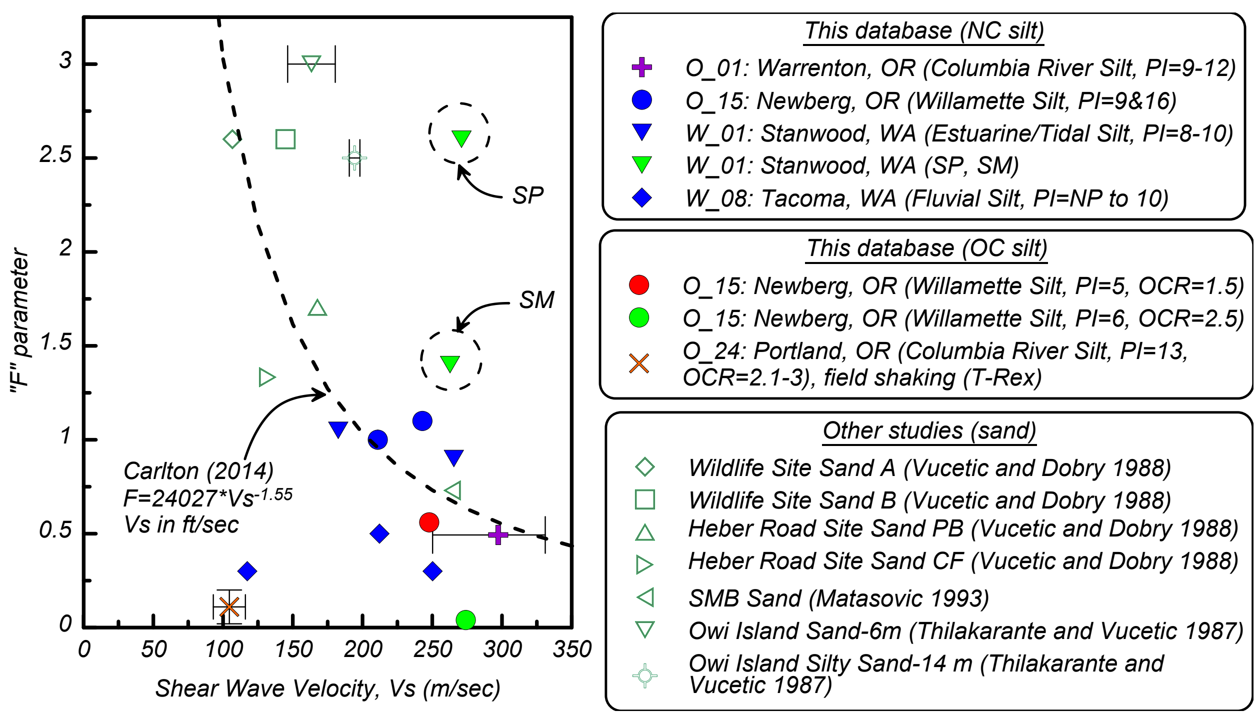

Figure 11: Variation between Parameter *F* in the Vucetic and Dobry model and the shear wave velocity (V_s).

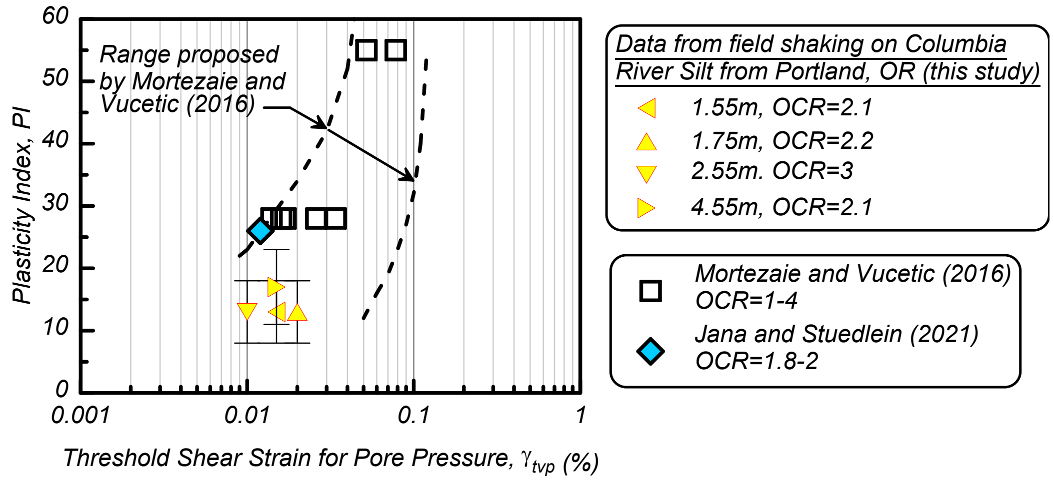

Figure 12. Comparison of threshold shear strain for cyclic pore water pressure generation (γ_{tp}) from this study and the data reported by Mortezaie and Vucetic (2016) and Jana and Stuedlein (2021).

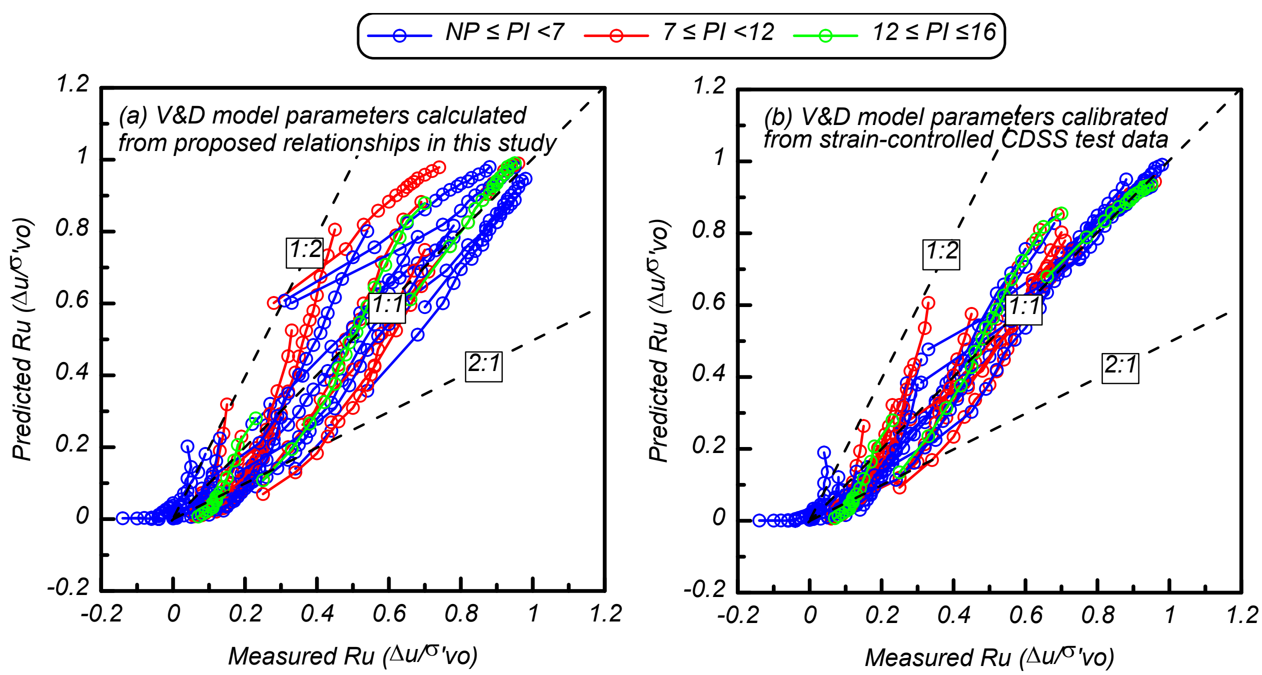

Figure 13: Comparison between measured and predicted pore pressure ratios for (a) V&D model parameters calculated using the proposed predictive equations in this study and (b) V&D model parameters calibrated based on the test data.